HNSJ Humanities & Natural Sciences Journal
ISSN: (e) 2709-0833
www.hnjournal.net
Peer-Reviewed Journal
Indexed at: NSP - SJIF
Impact Factor 2022 = 4.91

RESEARCH TITLE

Improving the Thermal and Electric Performance of Photovoltaic Panels Using Rear-Side Carbon Dioxide (CO_2) Gas Cooling

Basim Shehaib Jabur [1], Ahmed H. Yousif [2], Zaid M. H. Al-Dulaimi [3]

[1] *Department of Mechanical Engineering Techniques, AL–Qadisiyah Polytechnic College, AL-Furat AL- Awsat Technical University (ATU), Iraq*
[2] *Department of Mechanical Engineering Techniques, AL–Qadisiyah Polytechnic College, AL-Furat AL- Awsat Technical University (ATU), Iraq*
[3] *Engineering Technical College of Al-Najaf, Al-Furat Al-Awsat Technical University (ATU), Najaf, Iraq*
HNSJ, 2026, 7(9); https://doi.org/10.53796/hnsj79/50

Received at 15/08/2026 **Accepted at 22/08/2026** **Published at 01/09/2026**

Abstract

High operating temperatures, especially under high solar radiation and hot climate conditions, degrade the performance of photovoltaic (PV) panels significantly. Such an issue is specifically important for a country like Iraq; wherein high solar radiation availability assures a good prospect for renewable energy exploitation. Proper photovoltaic systems' establishment would not only lessen reliance on traditional energy sources but also sustainably support electricity generation in the nation. An increase in cell temperature leads to higher thermal losses and lowers the electrical output. This study presents the results of an experimental study carried out to enhance PV panel performance by rear surface cooling using injected carbon dioxide (CO_2) gas under different operating conditions. Two identical PV panels were used for the experimental work: one served as the reference panel (without cooling), while the other was used as the test panel with a rear-side cooling chamber. The effects of injection duration, mass flow rate, and injected gas temperature on the thermal and electrical performance of the PV panel were considered. Three injection durations were studied, 60, 90, and 120 seconds; three mass flow rates were 0.42, 0.54, and 0.675 g/s. The corresponding temperatures of the injected CO_2 were about −18 °C, −25 °C, and −35 °C, respectively. Results indicated that rear-surface cooling reduced the operating temperature of the PV panel and improved its electrical performance as compared to the case without cooling. An increase in injection duration enhanced thermal regulation of the panel, while an increase in mass flow rate improved convective heat transfer due to a larger amount of cold gas supplied to the rear surface. Best performance was obtained at the highest mass flow rate of 0.675 g/s and the longest injection duration of 120 seconds. In this condition, the cooling system provided optimal heat removal and, therefore, the highest improvement in electrical efficiency. Average electrical efficiency increased from 19.65% without cooling to 21.49% with cooling — an improvement of about 9.36%. It was also observed that cleaning mainly enhances optical performance while rear-surface cooling enhances thermal behavior; therefore, the combination of both can give better overall PV performance. The results confirm that rear-surface CO_2 cooling is a good approach to reduce thermal accumulation and enhance the power output and efficiency of photovoltaic panels.

Key Words: Photovoltaic module; Rear side cooling; Carbon dioxide; Electric efficiency; Gas cooling.

عنوان البحث

تحسين الأداء الحراري والكهربائي للألواح الكهروضوئية باستخدام التبريد بغاز ثاني أكسيد الكربون (CO_2) من الجانب الخلفي

المستخلص

تؤدي درجات حرارة التشغيل المرتفعة، ولا سيما في ظل الإشعاع الشمسي الشديد والظروف المناخية الحارة، إلى تدهور ملحوظ في أداء الألواح الكهروضوئية .(PV) وتكتسب هذه المشكلة أهمية خاصة في بلد مثل العراق، حيث يوفّر ارتفاع مستويات الإشعاع الشمسي فرصًا واعدة لاستغلال الطاقة المتجددة. ومن شأن إنشاء أنظمة كهروضوئية ملائمة أن يقلل الاعتماد على مصادر الطاقة التقليدية، فضلًا عن دعم توليد الكهرباء في البلاد بصورة مستدامة. وتؤدي زيادة درجة حرارة الخلايا إلى ارتفاع الفواقد الحرارية وانخفاض القدرة الكهربائية الناتجة. تعرض هذه الدراسة نتائج تجربة أُجريت لتحسين أداء الألواح الكهروضوئية من خلال تبريد سطحها الخلفي باستخدام غاز ثاني أكسيد الكربون (CO_2) المحقون تحت ظروف تشغيل مختلفة. استُخدم في التجربة لوحان كهروضوئيان متماثلان؛ استُخدم أحدهما بوصفه لوحًا مرجعيًا من دون تبريد، في حين استُخدم الآخر بوصفه لوحًا اختباريًا مزودًا بحجرة تبريد خلفية. ودُرست تأثيرات مدة الحقن، ومعدل التدفق الكتلي، ودرجة حرارة الغاز المحقون في الأداءين الحراري والكهربائي للوح الكهروضوئي. وشملت الدراسة ثلاث مدد للحقن، هي: 60 و90 و120 ثانية، وثلاثة معدلات للتدفق الكتلي، هي: 0.42 و0.54 و0.675 غرام/ثانية. وبلغت درجات حرارة غاز ثاني أكسيد الكربون المحقون المقابلة لهذه المعدلات نحو −18 و−25 و−35 درجة مئوية على التوالي. أظهرت النتائج أن تبريد السطح الخلفي أسهم في خفض درجة حرارة تشغيل اللوح الكهروضوئي وتحسين أدائه الكهربائي مقارنةً بحالة التشغيل من دون تبريد. كما أدى إطالة مدة الحقن إلى تعزيز التحكم الحراري في اللوح، في حين أسهمت زيادة معدل التدفق الكتلي في تحسين انتقال الحرارة بالحمل، نتيجة تزويد السطح الخلفي بكمية أكبر من الغاز البارد. وتحقق أفضل أداء عند أعلى معدل **للتدفق** الكتلي، البالغ 0.675 غرام/ثانية، وأطول مدة للحقن، البالغة 120 ثانية. وفي هذه الحالة، حقق نظام التبريد أفضل إزالة للحرارة، ومن ثم أعلى تحسن في الكفاءة الكهربائية. وارتفع متوسط الكفاءة الكهربائية من 19.65% من دون تبريد إلى 21.49% مع التبريد، أي بنسبة تحسن بلغت نحو 9.36%. ولوحظ أيضًا أن التنظيف يعزز الأداء البصري بصورة أساسية، في حين يحسن تبريد السطح الخلفي السلوك الحراري؛ ولذلك يمكن أن يؤدي الجمع بينهما إلى تحسين الأداء الكلي للألواح الكهروضوئية. وتؤكد النتائج أن التبريد الخلفي باستخدام غاز ثاني أكسيد الكربون يُعد نهجًا فعالًا للحد من التراكم الحراري وتعزيز القدرة الكهربائية الناتجة وكفاءة الألواح الكهروضوئية.

الكلمات المفتاحية: الوحدة الكهروضوئية؛ تبريد الجانب الخلفي؛ ثاني أكسيد الكربون؛ الكفاءة الكهربائية؛ التبريد بالغاز.

1. Introduction

Solar energy is a clean, safe and sustainable source for electrical power generation especially in countries with high solar irradiation as Iraq. In PV systems, the conversion of solar radiation to electrical energy is direct. The power produced is affected by several factors such as radiation intensity, conversion efficiency, location, panel orientation, tilt angle and weather conditions. Therefore, the improvement of the operating conditions of PV panels is essential to improve the electrical energy production (Abdulridha *et al.*, 2025).

Several PV cooling techniques have been investigated such as air cooling, water cooling, nanofluids, front- and rear-side cooling. Further exploration of the (CO_2) gas cooling under outdoor conditions is needed, since the rear-side cooling is beneficial for the PV performance (Nabil and Mansour, 2022).

Recent studies confirmed that PV efficiency decreases as cell temperature increases, which makes thermal management essential. Therefore, active cooling methods are needed to reduce module temperature, improve efficiency, and limit thermal degradation (Al Sadoon, Kassim and Mohmood, 2024).

Recent studies have confirmed that PV efficiency drops as the cell temperature increases, which makes thermal management a critical factor. Hence, active cooling techniques are required to reduce the temperature of the module, increase efficiency and avoid thermal degradation (Chaudhary *et al.*, 2024).

To keep higher power production and improve the system performance in outdoor conditions, the operating conditions of PV modules need to be improved. One of the main factors influencing the PV efficiency is the increase in temperature. Several cooling techniques have been studied to reduce the heat accumulation and to improve the thermal and electrical performance of photovoltaic modules (Al-jabari, Korkmaz and Teke, 2022).

2 Literature Review

2.1 Cooling method

PV cooling techniques can be classified into passive, active, and combined methods according to their operating mode and heat removal mechanism, as shown in figure 1. Passive methods use natural heat transfer without external power, while active methods require auxiliary energy to enhance cooling. Combined methods include features of both approaches to improve thermal performance while considering system complexity. (Harmailil *et al.*, 2024).

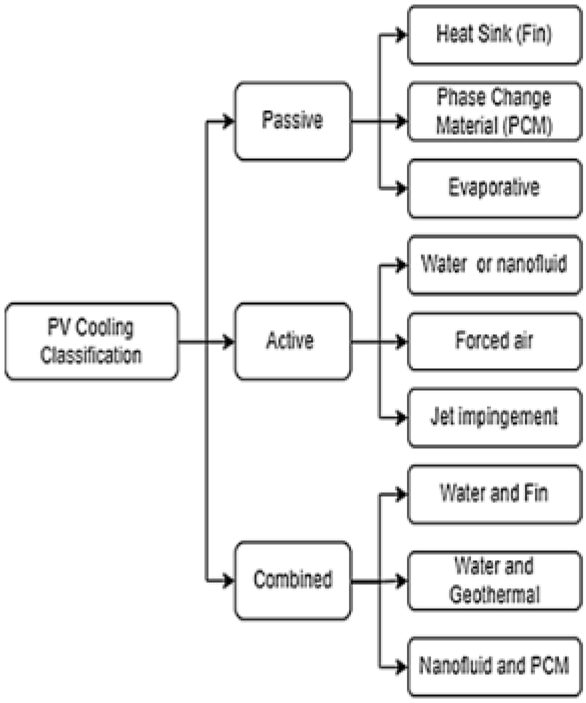

Figure 1: Classification of PV cooling method.

2.1.1 Passive

Passive fin cooling was studied by attaching aluminum fins on the rear surface of a PV module and comparing the performance with normal air cooling under ventilated and stagnant air conditions. The fins improved the convective heat transfer, reduced the maximum cell temperature by (3.7 ^{o}C), increased the electrical efficiency by (16.54%), and increased the thermal efficiency by (58.3%). The numerical results were in good agreement with the experimental validation (Abed, 2024).

rear-side paraffin wax phase change material (PCM) can effectively reduce PV module temperature under controlled laboratory conditions. The PCM cooling improved thermal stability, increased maximum power by about (1.35 W), and enhanced average efficiency by about (1.63%) (Xu *et al.*, 2023).

Passive cooling can reduce PV module temperature without any external power input.

This cooling method depends on natural heat dissipation by air or water, improves system reliability, and reduces operating cost, but its cooling effectiveness is lower than active techniques (Pichandi *et al.*, 2024).

A new passive thermal management design was proposed by integrating a PV module with a radiative cooling unit through a heat pipe. The PV–HP–RC system reduced the maximum operating temperature by about (12.86 ^{o}C) and increased the electrical efficiency by about (7.25%), showing the effectiveness of combining radiative cooling with heat pipe technology (Ahmed *et al.*, 2022).

Different types of phase change materials have been proposed for PV cooling to improve thermal regulation and electrical performance. Organic PCMs showed better performance than inorganic and eutectic materials due to their good thermal stability and latent heat properties, making them suitable for passive PV thermal management (Verma *et al.*, 2023).

Passive heat sinks with fins effectively reduced PV module temperature by more than (10 ºC), improving power output to over (90%) of the rated value. Furthermore, changing the fin inclination from (90º) to (45º) increased the power improvement from about (6.97%) to (7.55%), demonstrating the importance of fin geometry in passive PV cooling (Popovici *et al.*, 2016).

An aluminum plate was used as a base for passive PV cooling using PCM combined with micro heat sinks. The nanocomposite PCM (($RT44HC–Al_2O_3$)) with hollow cylindrical fins achieved a maximum temperature reduction improvement of (57.7%) using 22 fins and (0.77%) nanoparticle concentration, although this method increases system complexity and cost (Refaey *et al.*, 2021).

2.1.2 Active

A combined active cooling system using front-side water spraying and rear-side air cooling was developed for PV modules. The optimum case was obtained at an air flow rate of (0.25 kg/s), six nozzles, and a (30º) spray angle, reducing the panel temperature from (58 **ºC**) to (35 **ºC**), increasing output power by (24%), and improving efficiency from (9.78%) to (16.76%) (Jasim, 2023).

Different PV cooling methods were compared, including rear-side water cooling, rear-side nanofluid cooling, air cooling, and front-side water spraying. The results showed that front-side water spraying was the most effective method, reducing the panel temperature by (21.9%) and increasing the average daily electrical efficiency to (22%), with an improvement of (3.9%). Air cooling improved efficiency by only (1.1%), while rear-side water cooling and nanofluid cooling improved it by (1.9%) and (2.7%), respectively (Basem *et al.*, 2024).

A supercritical carbon dioxide ((CO_2))-based active cooling system was proposed for concentrated photovoltaic ((CPV)) cells using a heat sink with straight channels.

The (CO_2) cooling system improved thermal management by reducing the maximum cell temperature by about (4.3 K) and decreasing the temperature difference from (6.4 K) to (2.6 K). These results indicate that (CO_2) can be an effective alternative coolant for active PV thermal management, especially under high heat flux conditions (Mizani, Khoshvaght-aliabadi and Tae, 2025).

A hybrid PV/T solar evaporator using (CO_2) was developed as an active cooling system connected to a transcortical heat pump cycle. In this system, two-phase (CO_2) flows inside a serpentine stainless-steel tube bonded to the rear side of the solar absorber plate.

The results showed that (CO_2) cooling reduced the mean plate temperature by more than (25 ºC), increased electrical efficiency from (14.1%) to (16.0%), and produced about (1.028 kW) of useful thermal power (Paradis *et al.*, 2018).

A dual-source transcortical (CO_2) heat pump was experimentally investigated using PV/T collectors as direct-expansion evaporators. In solar-source mode, (CO_2) evaporates inside the rear tubes of the PV/T collectors, which cools the photovoltaic cells and improves their electrical production. The results showed that the solar-source mode increased the COP by up to (30%), while PV electrical production increased by about (10%) compared with the uncooled case (Zanetti, Azzolin, *et al.*, 2023).

A direct-expansion solar-assisted heat pump using (CO_2) was experimentally and numerically investigated with PVT collectors as evaporators. In solar mode, the (CO_2) refrigerant flows through the rear serpentine tubes of the PVT collectors, absorbing heat and cooling the photovoltaic cells. The results showed that this cooling improved photovoltaic electricity production by up to (8%), confirming the effectiveness of (CO_2)-based active cooling in PVT systems (Zanetti, Bordignon, *et al.*, 2023).

2.1.3 Combined (hybrid)

Hybrid PV cooling methods include nanoparticle-enhanced PCMs and biofluid-based cooling systems. Adding nanoparticles to PCM improves thermal conductivity, accelerates charging and discharging, and can increase electrical efficiency by up to (56%) and thermal storage by about (93%). Although hybrid systems provide better thermal and electrical performance than single cooling methods, material cost, system complexity, and long-term reliability must be considered (Prakash, Kukreja and Kumar, 2025).

Two PV cooling methods were compared: active water cooling and a hybrid system combining active water cooling with passive aluminum heat sink cooling.

The hybrid system improved heat removal from the rear surface and increased power output and electrical efficiency by (4.7%) and (0.84%), respectively, compared with (2.94%) and (0.52%) for active cooling alone. This indicates that combining passive elements with active cooling can enhance overall PV performance without full dependence on continuous active cooling (KARAOZAN and ASKER, 2023).

A hybrid water–air cooling system was developed to reduce and stabilize the operating temperature of PV modules under variable weather conditions. The system combined front-side water spraying with rear-side forced air cooling, which improved heat removal and produced more stable power than water cooling alone. The hybrid cooling increased PV power output by about (4.5%), showing a good balance between cooling effectiveness, water consumption, and system reliability (Azmi *et al.*, 2023).

A hybrid cooling system using dual thermoelectric coolers (TECs) was applied to the rear side of a PV module to improve heat removal. The system reduced the PV temperature by up to (17.27 ºC), increased electrical efficiency by (11.23%), and improved daily power output by about (8.3%) (Eid *et al.*, 2022).

A hybrid PV/T cooling system was developed using rear-side forced air cooling with front-side water cooling and self-cleaning. The system reduced the average PV temperature by about (15 ºC) compared with the uncooled reference case. At ($G=650$ W/m^2), the electrical efficiency increased by about (5.7%), while the total energy efficiency reached (85.3%), showing the effectiveness of combining air cooling, water cooling, and self-cleaning (Lebbi *et al.*, 2021).

3 Aim of the present study

The main objective of this study is to experimentally investigate the effect of rear-side (CO_2) gas cooling on the thermal and electrical performance of a photovoltaic module under outdoor conditions. The study aims to reduce the operating temperature of the PV module and improve its output power and electrical efficiency by using controlled (CO_2) injection at the rear surface.

4 Experimental Methodology

This study was carried out experimentally under outdoor operating conditions to investigate the effect of rear-side (CO_2) gas cooling on the thermal and electrical performance of a photovoltaic module. The general methodology of experimental work is presented in the flowchart shown in Fig. 2, which summarizes the main steps of the study, including system preparation, gas injection control, data measurement, and performance analysis.

Two identical monocrystalline PV modules were used in the experimental setup. One module was kept without cooling as a reference case, while the second module was modified with a rear-side (CO_2) cooling system. The complete experimental system is illustrated in Fig. 3, which shows the PV modules, supporting structure, (CO_2) cylinder, flow meter, control valve, gas distributor, and measuring instruments.

The cooled PV module was equipped with an aluminum chamber attached to its rear surface to allow (CO_2) gas to pass along the back side of the panel. The chamber was insulated using glass wool to reduce heat exchange with the surroundings. The (CO_2) gas was supplied from a cylinder and controlled using a solenoid valve connected to an Arduino system. During the tests, solar irradiance, ambient temperature, PV module temperature, and output power were recorded.

The collected data were used to compare the cooled and uncooled PV modules. Electrical efficiency, temperature reduction, power improvement, consumed (CO_2) mass, and heat removal rate were calculated to evaluate the effectiveness of rear-side (CO_2) gas cooling in improving PV performance under outdoor conditions.

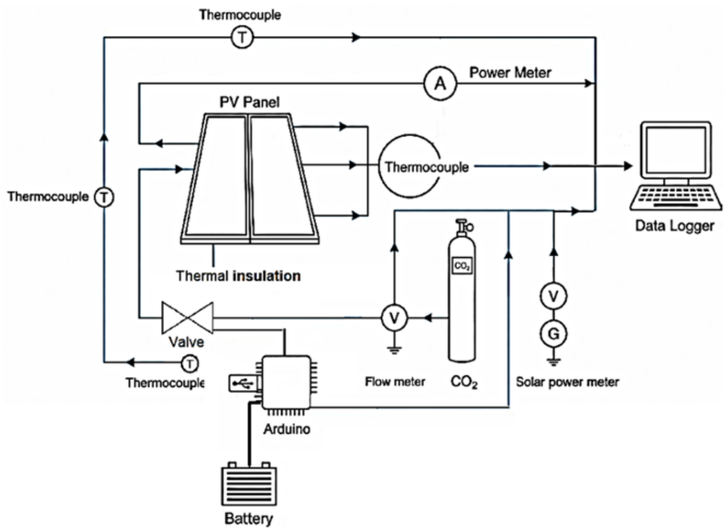

Figure 2 Schematic diagram of the Experimental setup used for rear-side CO_2 cooling of the photovoltaic module.

Figure 3 CO_2 gas supply line and distribution system used for rear side cooling of the photovoltaic module.

4.1 photovoltaic module and supporting structure

A monocrystalline photovoltaic module was employed as the primary energy conversion device in the experimental facility. Technical parameters of the PV module at rated power, electrical characteristics, efficiency, dimensions, operating temperature range, and maximum system voltage are described in Table (1). A flat plate photovoltaic module is usually tested on a flat surface so that it is subjected to the same conditions as those in actual use. In the present work, however, the photovoltaic module was mounted on a rigid steel support to ensure mechanical stability during the experimental tests. An additional steel angle was firmly fixed to the supporting frame to hold the module in position and stop any vibration, displacement, or change in orientation during the measurements. The module was mounted at a fixed tilt angle of 17^{o} from the horizontal plane so that it can receive suitable exposure to solar radiation for the testing duration. This mounting was necessary to provide stable conditions of operation so that meaningful comparison could be made between the clean uncooled reference case and the rear-side CO_2-cooled case.

Table (1). Technical specification of the photovoltaic module used in the experimental setup.

No.	Parameter	Value
1	Module type	Monocrystalline PV module
2	Maximum power	580 W
3	Maximum power voltage	43.20 V
4	Maximum power current	13.43 A
5	Open-circuit voltage	52.20 V
6	Short-circuit current	14.23 A
7	Module efficiency	22.50 %
8	Module dimensions	(2278*1134*30) mm
9	Maximum series fuse rating	25 A
10	Operating temperature range	(-40) to (+85) °C
11	Maximum system voltage	1500 V DC

4.2 Instrumentation and measurement tools

Several measuring instruments were used to record experimental data and evaluate the performance of the PV modules, as shown in figure 4. Three K-type thermocouples were attached to each PV module, for both the cooled and uncooled panels, to measure the operating temperature. These thermocouples were distributed in the upper, middle, and lower regions of the PV cell area to obtain a representative average module temperature. In addition, three external thermocouples were placed around the experimental setup to measure the ambient temperature. A solar power meter was used to measure the incident solar irradiance on the PV module surface. The electrical output power of each PV module was measured directly using a digital power meter. In addition, a (CO_2) flow meter was used to control and measure the volumetric flow rate of the injected gas before entering the rear cooling chamber. These instruments provided the required data for calculating temperature reduction, output power improvement, electrical efficiency, (CO_2) mass flow rate, consumed gas mass, and heat removal rate.

Figure 4. Experimental Measuring Instruments for PV Performance Evaluation.

4.3 CO_2 Mass flow rate and injection duration

The rear-side cooling experiments were carried out at three different CO_2 mass flow rates and three injection durations, i.e., (0.00042), (0.00054), and (0.000675) kg/s and 60, 90, and 120 s, respectively. These conditions were chosen to study the influence of these two parameters together on the thermal and electrical performance of the photovoltaic module. For every mass flow rate, CO_2 gas was injected into the rear-side cooling chamber for the duration specified. In this way, nine cooled test cases were obtained from the combination of the three mass flow rates and the three injection times. The calculated total injected CO_2 mass for each experimental case is presented in Table (2).

Table (2). CO_2 mass flow rate, injection duration, and total injection mass for the cooling test cases.

No.	Case	CO_2 mass flow rate Kg/s	Injection duration, (t) (s)
1	C_1	0.00042	60
2	C_2	0.00042	90
3	C_3	0.00042	120
4	C_4	0.00054	60
5	C_5	0.00054	90
6	C_6	0.00054	120
7	C_7	0.000675	60
8	C_8	0.000675	90
9	C_9	0.000675	120
10	C_{10}	0.00042	90, Cooled and unclean

4.4 Data reduction and performance calculations

The experimental data was processed to evaluate the thermal and electrical performance of the cooled and uncooled PV modules. The measured parameters included solar irradiance, PV module temperature, ambient temperature, electrical output power, (CO_2) volumetric flow rate, and injection duration. These data were used to calculate electrical efficiency, (CO_2) density, mass flow rate, consumed gas mass, heat removal rate, temperature reduction, and performance improvement.

Electrical efficiency was calculated using the following equation (1):(Chaudhary *et al.*, 2024)

$$\eta = \frac{P_{out}}{P_{in}} \times 100\ \%\ (1)$$

$$P_{in} = G\ \times A$$

A = panel area

Where: P_{in} (input power), P_{out} (output power), G (solar radiation intensity), and A (panel area)

The density of the CO_2 was calculated using the following equation (2):(Zhang *et al.*, 2024)

$$\rho = \frac{PM}{RT}\ (2)$$

Were

M=0.04401 Kg/mol

P= 101325 Pa

R=8.314 J / mol. K

$$\rho_{-18} = 2.1\ kg/m^3$$

$$\rho_{-25} = 2.16\ kg/m^3$$

$$\rho_{-35} = 2.25\ kg/m^3$$

The molar specific heat capacity was obtained from the following equation (3):(Tables, no date)

$$C_{p(mol)}\ a + bT + cT^2 + dT^3 \ (3)$$

Table (3) Symbol and units used the CO_2 Specific heat capacity calculation.

Type		Unit
a	First empirical coefficient	22.26
b	Second empirical coefficient	0.05981
c	Third empirical coefficient	-3.501×10^{-5}
d	Fourth empirical coefficient	7.469×10^{-9}

To convert:

$$C_{p(kg)} = \frac{C_{p(mol)}}{M}$$

$$C_{p(at-18\,kg)} = 0.798\ \frac{kJ}{kg\,.K}$$

$$C_{p(at-25\,kg)} = 0.791\ \frac{kJ}{kg\,.K}$$

$$C_{p(at-18\,kg)} = 0.779\ \frac{kJ}{kg\,.K}$$

The corresponding mass flow rate was calculated according to the following relation, where the flow meter readings were proportional to the gas flow through the supply line (4):(Tables, no date)

$$\dot{m} \ = \dot{V} \times \rho \ (4)$$

12 L/m = 0.0002 m^3/s

15 L/m = 0.000254 m^3/s

18 L/m = 0.00030 m^3/s

$$\dot{m}_1 = 0.0002 \times 2.1 = 0.00042\ \frac{kg}{s}$$

$$\dot{m}_2 = 0.000254 \times 2.16 = 0.00054\ \frac{kg}{s}$$

$$\dot{m}_3 = 0.00030 \times 2.25 = 0.000675\ \frac{kg}{s}$$

The specific heat capacity of the gas and the temperature difference between the outlet and inlet gas temperatures (Jain *et al.*, 2026).

The heat removal rate was calculated as follows:

$\dot{Q} = \dot{m}\, C_p\, \Delta T$ (5)

$\Delta T = T_{out} - T_{in}$

LIST OF SYMBOLS AND ABBREVIATIONS

Symbols	Meaning	Units
ρ	Density	kg/m³
P	Pressure	Pa
M	Molar mass	kg/mol
R	Universal gas constant	8.314 J/mol. K
C_p (mol)	Molar specific heat at constant pressure	J/mol· K
C_p	Specific heat at constant pressure on a mass basis	J/kg· K
T	Absolute temperature	(K)
$\dot{m}$	mass flow rate	kg/s
$\dot{V}$	volumetric flow rate	m³/s
Q	Heat transfer rate	W/s or kW/s
C_p	Specific heat capacity at constant pressure	J/kg·°C or J/kg· K
ΔT	Change in temperature	°C or K

5 RESULTS AND DISCUSSIONS

5.1 Thermal performance of rear surface cooling

Figure 4 shows the rear-surface temperature variation of the uncooled and (CO_2)-cooled PV modules at a mass flow rate of (0.00042 kg/s) and an injection duration of (60 s). The temperature increased gradually during the morning and reached its maximum value around 1:00 PM due to the increase in solar irradiance. The uncooled module reached about (89 °C), while the cooled module reached (85.6 °C), giving a maximum temperature reduction of about (3.4 °C). This reduction is attributed to the flow of relatively cold CO_2) gas along the rear surface, which absorbed part of the accumulated heat and removed it from the panel. Although the reduction was limited, the cooled module maintained a lower temperature than the uncooled module during most of the test period, confirming the positive effect of (60 s) rear-side (CO_2) injection on PV thermal behavior.

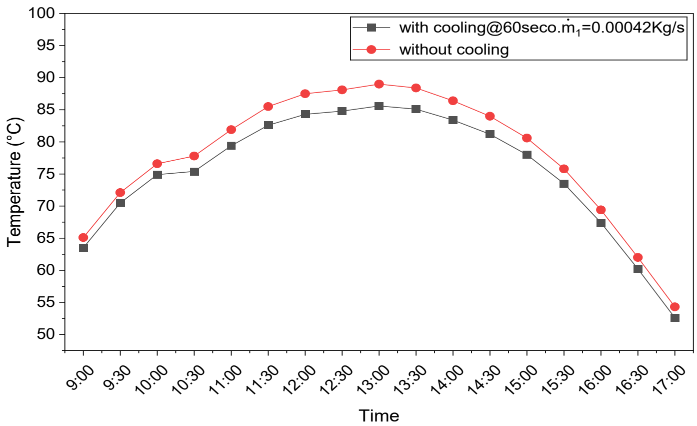

Figure 4. rear surface temperature variation with time under cooled and uncooled conditions.

Figure 5 shows the rear-surface temperature variation of the uncooled and (CO_2)-cooled PV modules. The test was conducted at a mass flow rate of (0.00042 kg/s) and an injection duration of (90 s). In both cases, the temperature increased gradually during the morning and reached higher values around noon. The uncooled module recorded a maximum temperature of about (73 ºC) at 12:00 PM. The cooled module reached a maximum temperature of about (67.1 ºC) at 1:00 PM. The maximum temperature reduction was about (6.5 ºC), while the average reduction was (4.65 ºC). This improvement is due to the larger amount of (CO_2) injected during the (90 s) period, which enhanced heat removal. Therefore, rear-side (CO_2) cooling at (90 s) provided better thermal regulation than the uncooled case.

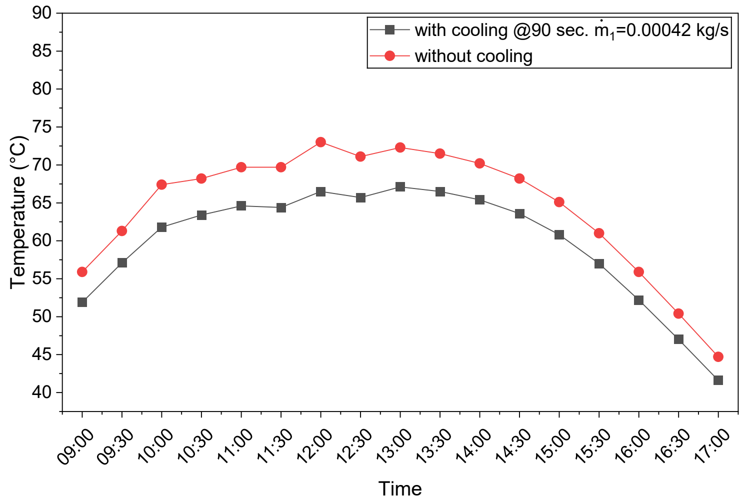

Figure 5. rear surface temperature variation with time under cooled and uncooled conditions.

The rear surface temperature of the photovoltaic panel was taken vs. time for both uncooled and cooled cases as shown in Figure 6. This cooling was performed by giving an injection duration of 120 seconds at a mass flow rate of 0.00042 kg/s. From the results, it was noted that, in the morning hours, the rear surface temperature increased slowly until 1:00 PM, attaining a value of 71.1 °C for the uncooled panel and 64.4 °C for the cooled panel at this time. Throughout the test period, the maximum temperature of the rear surface for the uncooled panel was higher than that for the cooled panel. It was about 6.8 °C at 12:30 PM maximum reduction whereas the average reduction was approximately 6.15 °C. The improvement is due to the longer injection time, which increased the amount of released CO_2 gas and the heat removal from the PV module back surface.

Therefore, the best thermal control of the cases tested was achieved with rear-surface cooling and 120 seconds of injection duration, which also helped to keep the rear surface temperature at a lower level.

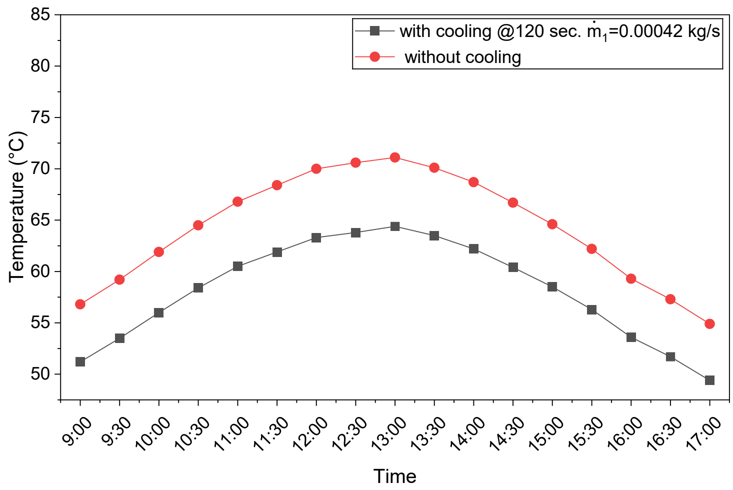

Figure 6. rear surface temperature variation with time under cooled and uncooled conditions.

5.2 Effect of injection duration on panel temperature

The effect of increasing the duration of CO 2 injection from 60 s to 120 s on the reduction of rear-surface temperature of the photovoltaic panel is shown in Figures 4.3, 4.4 and 4.5. When the injection duration was 60 s, the cooling effect was limited, with the maximum temperature reduction of about 3.4 °C, and the average reduction being 2.48 °C. The increase of injection duration to 90 s resulted in the increase of the amount of discharged CO2 gas and the improvement of the heat removal from the rear surface. Consequently, the maximum temperature reduction increased to approximately 6.5 °C and the average temperature reduction was 4.65 °C.

The optimum cooling behavior was achieved at 120 s of injection duration. Here the maximum reduction of temperature was about 6.8 °C and the average reduction was 6.15 °C. The maximum temperature reduction was only slightly higher at 120 s than at 90 s, but the average temperature reduction was clearly better. This suggests that the 120 s injection duration resulted in more consistent cooling over the test period rather than a brief period of temperature reduction. Thus, the injection duration of 120s can be considered as the best case for the thermal regulation of the PV rear surface. However, the 90 s injection duration may be a practical compromise between cooling improvement and CO2 gas consumption.

5.3 Effect of mass flow rate on panel temperature

The results of the rear surface temperature of the photovoltaic panel with time at different mass flow rates under the same injection duration of 60 seconds are shown in Figure 7. Three mass flow rates, 0.00042 kg/s, 0.00054 kg/s, and 0.000675 kg/s were tested. It was observed that, in general, the rear surface temperature increased slowly during the morning hours to reach the maximum value around noon and early afternoon. For the 0.00042 kg/s mass flow rate, the highest temperature was attained and was 85.6 °C at 1:00 PM. For the other two mass flow rates of 0.00054 kg/s and 0.000675 kg/s, the maximum temperatures were 75.2 °C and 68.7 °C, respectively. The results of this study clearly indicate that the improvement of the cooling performance of the rear surface is achieved with an increase in the mass flow rate. This behavior can be attributed to the larger amount of cooling fluid that passes over the rear surface of the PV panel, which enhances convective heat transfer and thus limits the rise in temperature. The average temperature of the rear surface dropped from about 75.44 °C at 0.00042 kg/s to 65.16 °C at 0.00054 kg/s and then to 58.89 °C at 0.000675 kg/s. Therefore, the highest mass flow rate gave the best thermal regulation under the 60-second injection condition.

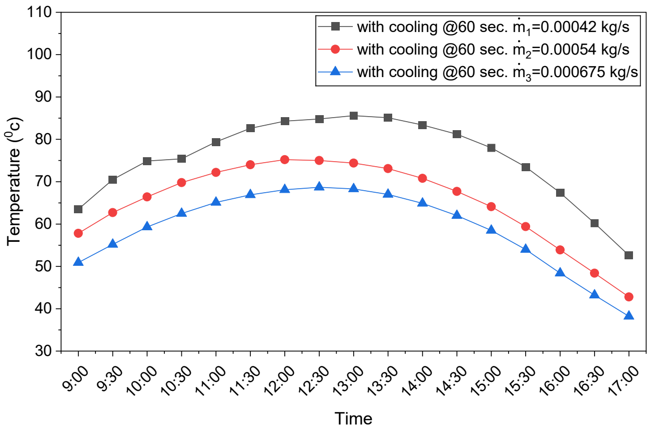

Figure 7. Rear surface temperature variation with time at different mass flow rate.

Figure 8 shows the rear surface temperature results for the photovoltaic panel over time for different mass flow rates with an injection duration of 90 seconds. Three mass flow rates of 0.00042 kg/s, 0.00054 kg/s, and 0.000675 kg/s were tested. The rear surface temperature was observed to increase gradually in the morning hours until it reached maximum values around noon and early afternoon. For a mass flow rate of 0.00042 kg/s, the maximum temperature was found to be 67.1 °C at 1:00 PM. For the other two mass flow rates, the maximum temperatures were 65.3 °C and 61.0 °C, respectively. This result proves that increasing the mass flow rate enhances the cooling performance of the rear surface. This can be due to the higher amount of cooling liquid passing over the rear surface, which increased the contact between the liquid and the heated surface and enhanced the cooling effect. The average rear surface temperature dropped from around 59.80 °C at 0.00042 kg/s to 55.67 °C at 0.00054 kg/s, and then to 51.24 °C at 0.000675 kg/s. Thus, the highest mass flow rate gave the best thermal regulation under the 90-second injection condition.

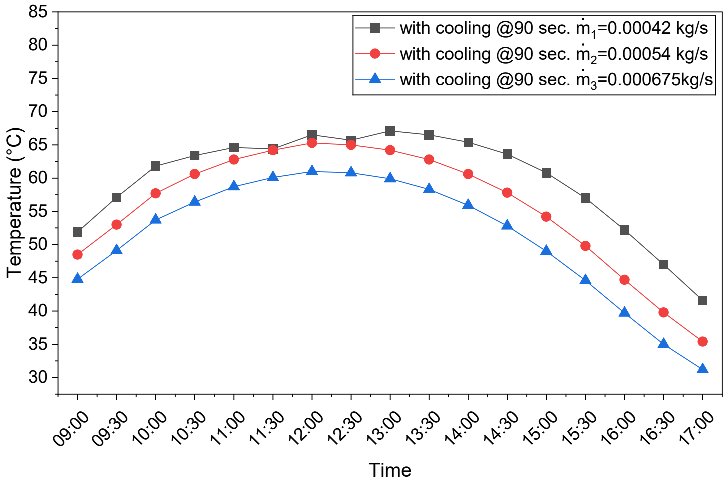

Figure 8. Effect of mass flow rate on rear surface temperature at 90- second injection duration.

Fig. 9 shows the effect of (CO_2) mass flow rate on the rear-surface temperature of the photovoltaic panel with fixed injection duration of 120 s. Three mass flow rates were experimented (0.00042), (0.00054) and (0.000675 kg/s). The rear surface temperatures for the three mass flow rates were close to each other in the morning hours. This behavior can be explained by the lower thermal load in the first test phase, where the panel temperature was still slowly increasing and heat accumulation was limited. Therefore, the difference in heat removal between the three mass flow rates before noon was not clearly visible. As time approached noon and the early afternoon period, solar radiation and ambient temperature increased, which resulted in a greater accumulation of heat in the PV module. In these conditions the effect of mass flow rate was more pronounced. A higher mass flow rate of (CO_2) enabled more of the cooling gas to flow over the rear surface, therefore enhancing the heat removal rate and lowering the rear-surface temperature more efficiently. Therefore, the temperature curves diverged after midday, especially at the highest mass flow rate (0.000675 kg/s). At the lowest mass flow rate of (0.00042 kg/s), the rear-surface temperature reached about (64.4 ºC) at around 1:00 PM, while it decreased to about (63.8 ºC) at (0.00054 kg/s) and further to (58.0 ºC) at (0.000675 kg/s). The average temperature on the rear surface was (58.15 ºC) at (0.00042 kg/s) and then decreased to (54.16 ºC) at (0.00054 kg/s) and (48.71^\circ C) at (0.000675 kg/s). These results show that the cooling performance is improved by increasing the mass flow rate, especially in the period of high thermal load. The best thermal regulation of the PV rear surface was demonstrated at the highest mass flow rate.

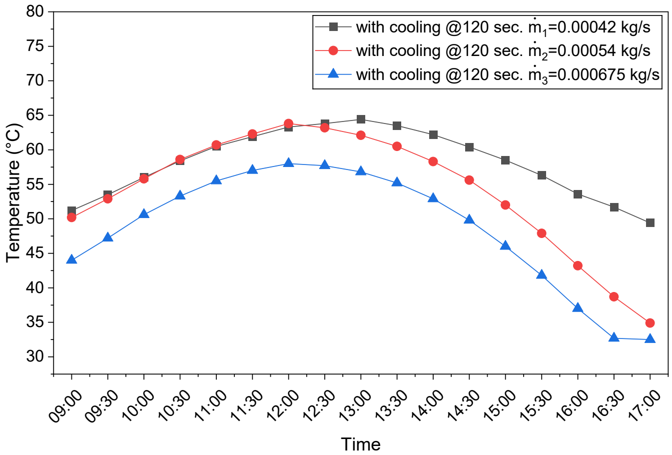

Figure 9. Effect of mass flow rate on rear surface temperature at 120- second injection duration.

5.4 Effect of injection duration at constant mass flow rate

This is shown in Figure 10. Constant rear surface temperature of the photovoltaic panel for a mass flow rate of 0.00054 kg/s Studied injection times were 60 seconds, 90 seconds and 120 seconds. The back face temperatures increased gradually in the morning up to maximum values around 12:30 PM, then started to decrease in the afternoon due to reduction of the solar radiation. The maximum back face temperature for the 60 s injection duration was 75.2 °C. It then decreased to 65.3°C and 63.8°C for the injection durations of 90s and 120s, respectively. The results show that the cooling performance of rear surface is improved with the increase of injection duration. This is because the injection period is longer, so that the cooling fluid has more time to contact the heated rear surface and the cooling effects are improved, and the temperature rise is reduced. The average rear surface temperature was reduced from approximately 65.16 °C at 60 seconds to 55.67 °C at 90 seconds and 54.16 °C at 120 seconds. The 120-second case showed the lowest average temperature, but the difference with the 90-second case was rather small. So, the thermal performance was best for 120 second injection duration. However, the 90 seconds duration could be considered as a quite practical option in the trade-off between the cooling performance and the coolant consumption.

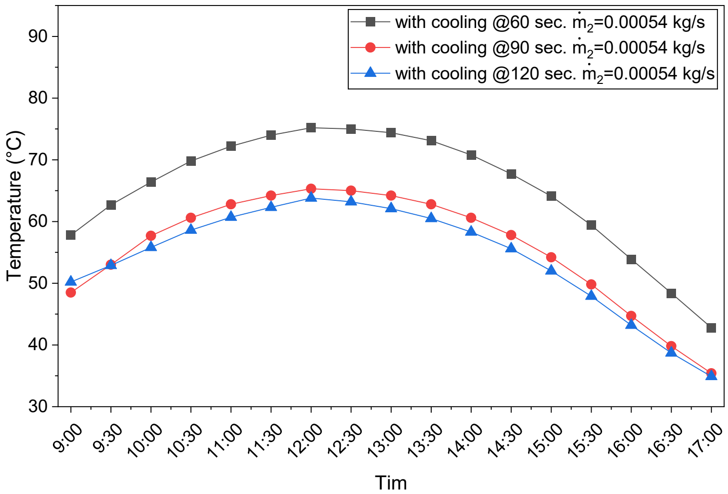

Figure 10. Effect of injection duration on rear surface temperature at a mass flow rate of 0.00054 Kg/s

5.5 Electrical power performance analysis

Results showing the variation of electrical output power for the photovoltaic panel with time under cooled and uncooled conditions, at an injection duration of 60 seconds and a mass flow rate of 0.00042 kg/s, are presented in Figure 11. The results illustrate how electrical power increased gradually during the morning hours, along with solar radiation, and reached its maximum value at 1:00 PM. At that time, the cooled panel produced 485 W, while the uncooled panel produced 458.3 W. Throughout the testing period, therefore, electrical power under the cooled condition was higher than that of the uncooled condition. The improvement can be ascribed to the fact that rear-surface cooling reduced the panel temperature and, thus, limited heat buildup while enhancing the thermal operating condition of the PV cells. Maximum power enhancement was about 26.7 W at 1:00 PM. Average power increase was approximately 20.82 W - an average improvement of about 5.27% over the uncooled case. That said, rear-surface cooling, with a 60-second injection duration, helped boost electrical power output for the photovoltaic panel.

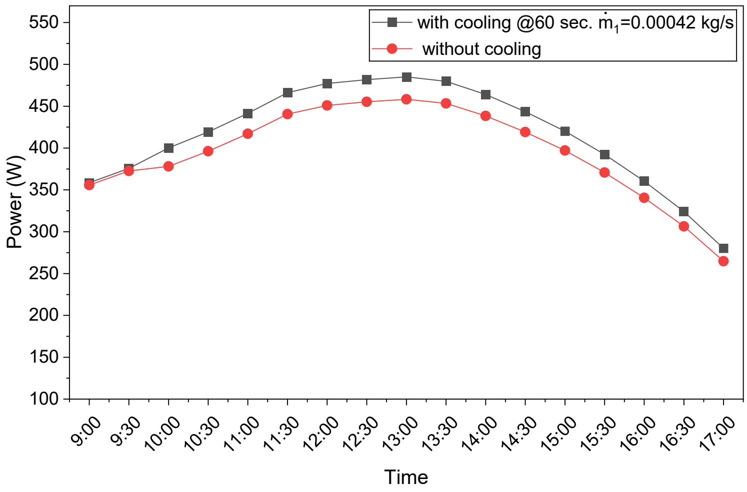

Figure 11 Electrical power variation with time under cooled and uncooled condition at 60 - second.

The results of the electrical output power of the photovoltaic panel with time for cooled and uncooled conditions at an injection duration of 90 seconds and a mass flow rate of 0.00042 kg/s are shown in Figure 12. The output power increased gradually in the morning hours due to solar radiation and reached its maximum value at 12:00 PM; at this instant, the cooled panel was giving 515 W while the uncooled one was giving 481.5 W. Throughout the testing period, the results indicated that the cooled panel provided higher electrical power than the uncooled panel. This enhancement is primarily since the rear surface temperature was reduced as a result of the cooling process. In this case, when the cooling fluid was directed to the rear surface, it also helped to minimize the thermal effect on the PV cells; hence, it improved the operating condition of the panel and increased the power output. The maximum enhancement in power was about 33.5 W at 12:00 PM. The average increase in power was approximately 26.13 W, which corresponds to an average improvement of about 7.0% compared with the uncooled case. Hence, rear-surface cooling with a 90-second injection duration proves to have improved the electrical power output of the photovoltaic panel.

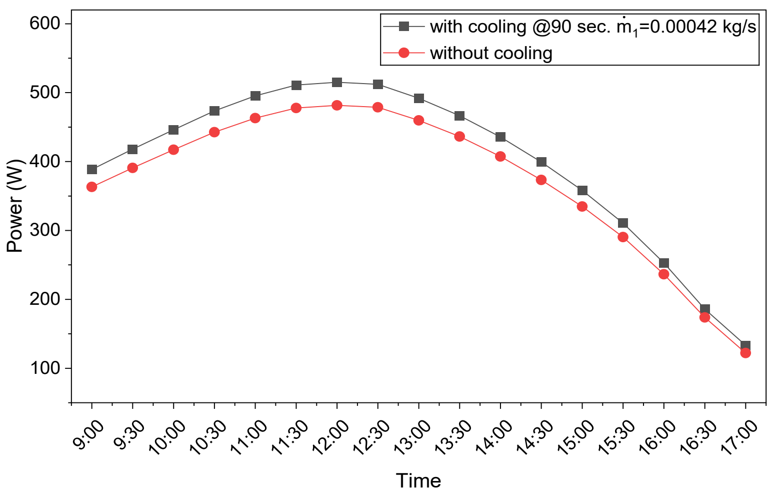

Figure 12 Electrical power variation with time under cooled and uncooled condition at 90 - second.

The results in Figure 13 show the variation of electrical output power of the photovoltaic panel with time for cooled and uncooled cases at an injection duration of 120 seconds and a mass flow rate of 0.00042 kg/s. The electrical power increased gradually in the morning hours with increasing solar radiation to reach its maximum value at 12:00 PM. At this time, it was 545 W for the cooled panel and 501.4 W for the uncooled panel. The electrical power was always higher under cooled conditions than under uncooled conditions during the entire period of the test. This enhancement is due to the longer injection duration that improved the rear-surface cooling effect and reduced the operating temperature of the PV panel, hence better thermal conditions for the solar cells which lead to higher electrical power output. Pmax enhancement was ~43.6 W at 12:00 PM, and the average enhancement of power was approximately ~32.55 W, which corresponds to an average improvement of ~8.64% compared to the uncooled case. Hence, rear surface cooling with an injection duration of 120 seconds is a clear enhancement of the electrical output power of the photovoltaic panel over that of the uncooled case.

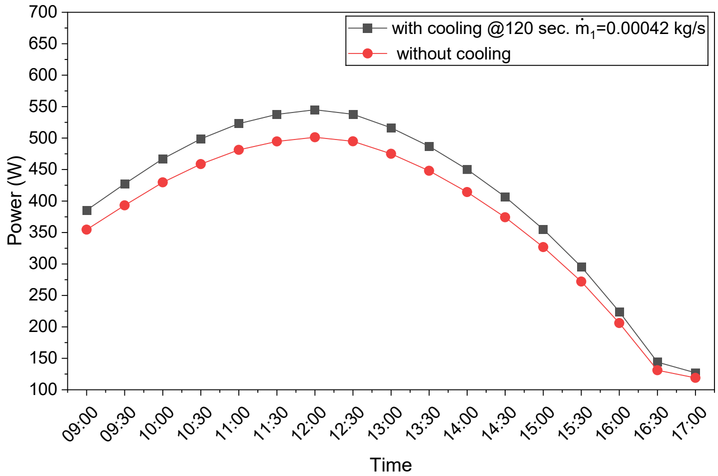

Figure 13. Electrical power variation with time under cooled and uncooled condition at 120 - second.

5.6 Effect of mass flow rate on electrical output power

The results of the effect of mass flow rate of the cooling fluid on the electrical output power of the photovoltaic panel at an injection duration of 60 seconds are shown in figure 14. Three mass flow rates were considered, $\dot{m}_1$= 0.00042 kg/s, $\dot{m}_2$= 0.00054 kg/s, $\dot{m}_3$= 0.000675 kg/s. It was observed that the electrical power increased gradually from the beginning of the day as solar radiation started to increase and reached a maximum value at noon. The maximum power registered was 485W at m1, increasing to 495W at $\dot{m}_2$ and further to 515W at $\dot{m}_3$, showing that as the mass flow rate increased, there was better cooling which improved the electrical power output. Most of this improvement was due to more cooling fluid available to pass over the rear surface of the PV panel. This in turn decreases the temperature of the panel, thus giving good thermal operating conditions for the solar cells.

But there was a significant drop in power around 16:00, especially at $\dot{m}_2$ and $\dot{m}_3$. The decrease can be explained by the decrease in the solar radiation in the late afternoon, due to the lower solar altitude and higher incidence angle. But for higher mass flow rates better cooling is obtained. But by this time the available solar energy is much lower. So, the cooling effect cannot compensate for the reduction in the solar radiation incident. Thus, the results indicate that $\dot{m}_3$=0.000675kg/s provided the best electrical performance under the 60s injection condition and the power drop at 16:00 is mainly due to the decrease of solar irradiance rather than the cooling performance flaw.

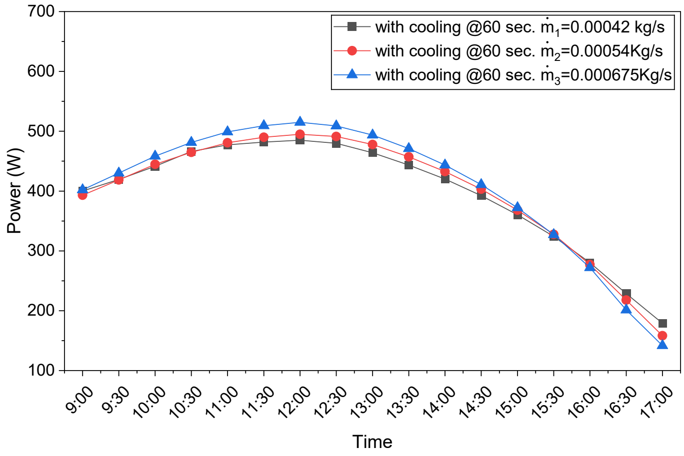

Figure 14. Effect of mass flow rate on electrical output power at 60 – second injection duration.

Figure 15 also presents the results of varying mass flow rate on electrical output power of the photovoltaic panel at an injection duration of 90 seconds. Three mass flow rates considered were $\dot{m}_1$ = 0.00042 kg/s, $\dot{m}_2$ = 0.00054 kg/s, and $\dot{m}_3$ = 0.000675 kg/s. The power output slowly increased in the morning with solar radiation until it reached its maximum value at noon. The maximum power was recorded as 515 W at $\dot{m}_1$, 530 W at $\dot{m}_2$, and 542 W at $\dot{m}_3$. Thus, an increase in mass flow rate improved cooling performance and enhanced electrical output. This enhancement is due to more cooling fluid crossing over the rear surface of the PV panel reducing heat accumulation and thus improving thermal operating condition of solar cells. The average power output increased from about 399.62 W at $\dot{m}_1$ to 411.29 W at $\dot{m}_2$ and then to 416.15 W at $\dot{m}_3$. However, a great drop in power is realized during the late afternoon, especially around 16:00, because solar radiation seriously falls as the solar altitude lowers and the angle of incidence increases. Thus, while the higher mass flow rate avails better cooling, the solar energy available is not enough to sustain the high-power levels seen around noon. In general, $\dot{m}_3$ = 0.000675 kg/s offered the best electrical performance under the 90-second injection condition.

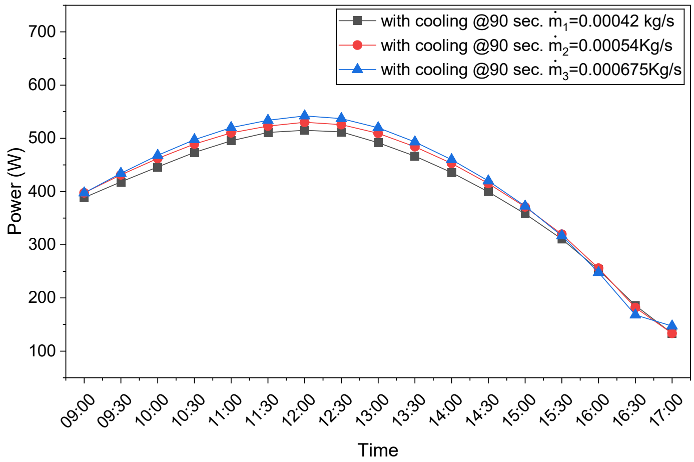

Figure 15. Effect of mass flow rate on electrical output power at 90 – second injection duration.

Figure 16 illustrates the effect of mass flow rate of the cooling fluid on the electrical output power of the photovoltaic panel at a constant injection duration of 120 seconds. Three mass flow rates $\dot{m}_1$ = 0.00042 kg/s, $\dot{m}_2$ = 0.00054 kg/s, and $\dot{m}_3$ = 0.000675 kg/s were considered. The electrical power increased gradually in the morning hours with the increase in solar radiation and reached its maximum value at 12:00 PM. The output power was 545 W, 556 W, and 568 W for $\dot{m}_1$, $\dot{m}_2$, and $\dot{m}_3$, respectively. This indicates that increasing the mass flow rate enhanced the rear-surface cooling effect and therefore improved the electrical output during the period of high solar radiation. However, there was also some convergence between some values in the afternoon after 3:30 PM. In particular, the output power at $\dot{m}_2$ and $\dot{m}_3$ became very close, and in some periods $\dot{m}_3$was slightly lower than $\dot{m}_2$, such as at 3:30 PM, 4:00 PM, and 4:30 PM. This behavior can be scientifically explained by the dominance of solar irradiance reduction in the late afternoon. As the solar altitude decreases and the angle of incidence increases, the available solar energy received by the PV panel becomes significantly lower. Therefore, although the higher mass flow rate provides better cooling, the additional cooling effect becomes less influential when the incident solar radiation is low. The convergence or slight overlap between the values may also be related to the reduced temperature difference between the tested cases under low-radiation conditions, in addition to minor experimental fluctuations within the measurement range. In general, the best performance was delivered by a mass flow rate of 0.000675 kg/s during the high-radiation period, while the difference between the mass flow rates became less significant in the late afternoon due to the sharp reduction in solar irradiance.

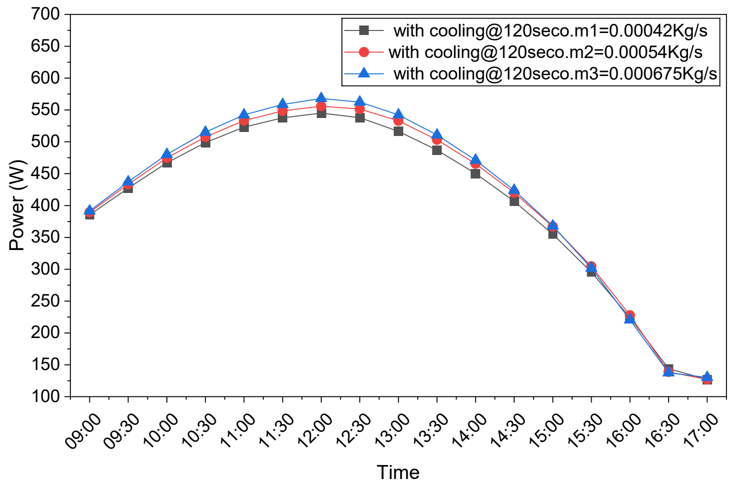

Figure 16. Effect of mass flow rate on electrical output power at 120 – second injection duration.

5.7 Effect of injection duration on electrical output power

The effect of the injection duration on the electrical output power of the photovoltaic panel at a constant (CO_2) mass flow rate of $\dot{m}_2$=0.00054 kg/s) is shown in Figure 17. Injection durations of 60 s, 90 s and 120 s were examined. Generally, solar irradiance increased gradually during the morning hours, and the electrical output power increased gradually and obtained its maximum value at noon.

The maximum output power was approximately 495 W at 60 s, increased to 530 W at 90 s, and reached 556 W at 120 s. This suggests that the rear-surface cooling effect during the high-radiation period was improved by extending the injection duration, resulting in a decrease in the panel temperature and an increase in the electrical output power. This enhancement is attributed to the increased quantity of discharged (CO_2) gas at longer injection times that resulted in the increased heat removal from the rear surface of the PV panel. Thus, the adverse effect of temperature rise on the solar cells was mitigated. The average power increased from around 399.89 W at 60 s to 411.29 W at 90 s and 416.55 W at 120 s. Around 2:30 PM the difference between the three cases was reduced and the curves started to converge and partially overlap.

This behavior does not imply that the longer injection duration was less effective in terms of thermal. Instead, it shows that the electrical power output in the late afternoon was mainly determined by the reduction of solar irradiance and the change in the sun angle. During this period, the available solar energy reaching the PV panel dropped rapidly, so that the additional cooling effect could not compensate for the reduction of incident solar radiation. Some values were close or slightly changed in order between the three-injection duration. The best electrical performance was obtained with the injection duration of 120 s especially during the high solar radiation period. However, the injection duration of 90 s can be considered as a practical compromise between electrical power improvement and (CO_2) gas consumption.

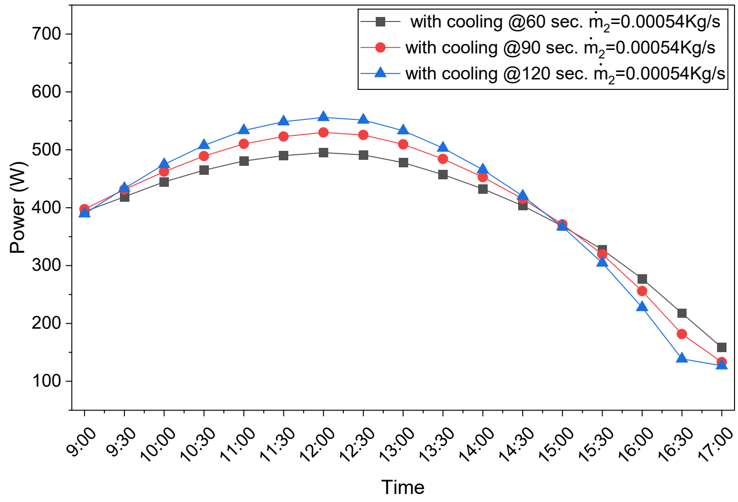

Figure 17 Effect of injection duration on electrical output power at $\dot{m}_2$=0.00054 Kg/s.

5.8 Heat removal rate analysis

From Figure 18, one can see that there is a big difference in the rate of removing heat, Q, for low mass flow rate m1 and the higher mass flow rate $\dot{m}_2$ and $\dot{m}_3$. This difference should be due to the combined effect of mass flow rate and injected gas temperature. At $\dot{m}_1$ = 0.00042 kg/s, the temperature of the injected gas was −18 °C, and it decreased to −25 °C at $\dot{m}_2$ = 0.00054 kg/s before reaching −35 °C at $\dot{m}_3$ = 0.000675 kg/s. In this case, therefore, the mass flow rate was increased as the injected gas temperature decreased, which then increased the temperature difference between the heated rear surface of the PV panel and the cold gas; hence, it enhanced the driving force for convective heat transfer. At $\dot{m}_1$, the gas passes over the rear surface with relatively low amount, and the temperature difference between the gas and the heated surface is smaller compared to the other two cases. As a result, the gas ability to absorb and remove heat from the panel is reduced. On the other hand, at $\dot{m}_2$ and particularly at $\dot{m}_3$, the higher mass flow rate provides a larger amount of cooling gas in the same duration of injection over which the lower gas temperature increases the effective thermal gradient between the fluid and the surface. Consequently, convective heat transfer is enhanced, leading to a noticeable increase in Q.

This is because the better thermal performance recorded at $\dot{m}_3$ results not only from the higher mass flow rate but also from the combination of the highest flow rate and the lowest injected gas temperature, which gave the most favorable conditions for removing heat from the rear surface of the photovoltaic panel.

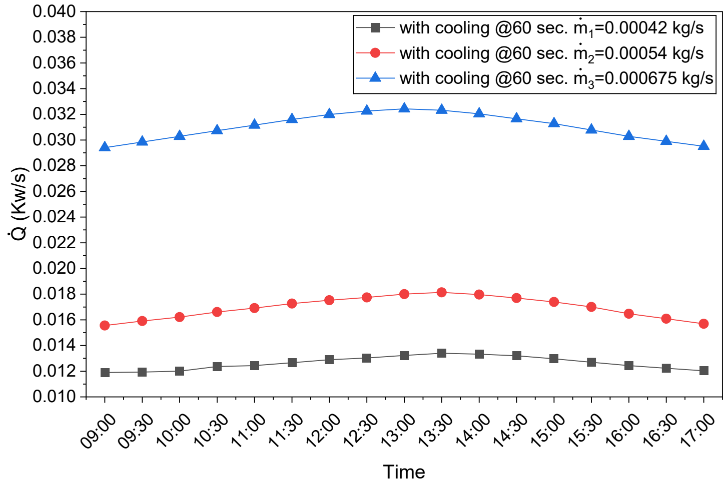

Figurer 18. Effect of mass flow rate on heat removal rate at 60 – second injection duration

The results in Figure 19 below show the effect of mass flow rate on the heat removal rate Q for an injection duration of 90 seconds. Three mass flow rates were considered in this case, namely; $\dot{m}_1$ = 0.00042 kg/s, $\dot{m}_2$ = 0.00054 kg/s, and $\dot{m}_3$ = 0.000675 kg/s. Generally, the heat removal rate increased gradually during the morning hours to attain its maximum value around 1:00 PM. The maximum values of Q were 0.02658 kW/s, 0.03437 kW/s, and 0.04129 kW/s for $\dot{m}_1$, $\dot{m}_2$, and $\dot{m}_3$, respectively. This shows that an increase in mass flow rate enhances the thermal performance of the rear surface cooling system. The higher values of Q at m2 and m3 are explained by the combined effect of higher mass flow rate and lower injected gas temperature. The temperature of the injected gas was −18 °C at $\dot{m}_1$ and decreased to −25 °C at $\dot{m}_2$ and further to −35 °C at $\dot{m}_3$. As a result, the temperature difference between the hot rear surface and the cooling gas increased, which further enhanced the driving force for convective heat transfer. Besides, the higher flow rate would allow a larger amount of cooling gas to pass over the rear surface in the same injection period, thereby increasing the ability of the gas to absorb and carry heat away from the panel. Therefore, $\dot{m}_3$ achieved the highest average heat removal rate, about 0.03761 kW/s, compared with 0.03143 kW/s for $\dot{m}_2$ and 0.02437 kW/s for $\dot{m}_1$. The results, in general, confirm that the best thermal performance at the 90-second injection duration was obtained at a mass flow rate of $\dot{m}_3$ = 0.000675 kg/s, due to the combination of the highest mass flow rate and the lowest injected gas temperature.

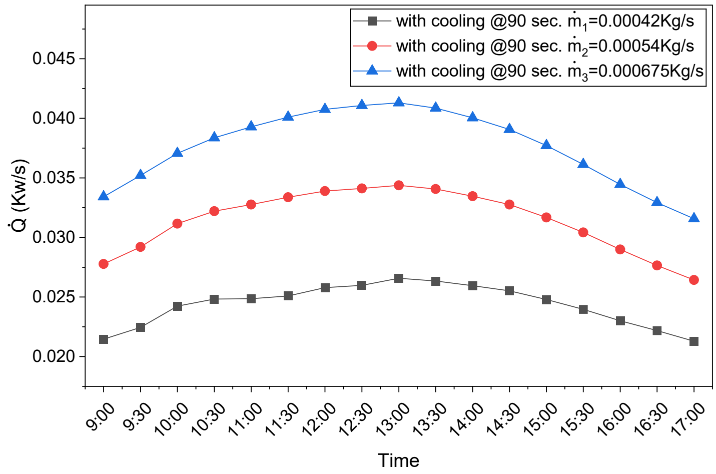

Figure 19. Effect of mass flow rate on heat removal rate at 90 – second injection duration.

The results in Figure 20 below show fluctuations in the heat removal rate Q are obvious at the low mass flow rate $\dot{m}_1$ = 0.00042 kg/s as compared to $\dot{m}_2$ and $\dot{m}_3$. This can be attributed to the fact that only a small amount of gas is injected at $\dot{m}_1$, and it enters at a relatively higher temperature of −18 °C, as compared to −25 °C at $\dot{m}_2$ and −35 °C at $\dot{m}_3$. As a result, the temperature difference between the cooling gas and the heated rear surface becomes less, which makes the driving force for heat transfer also less; thus, the cooling process becomes more sensitive to instantaneous changes in solar radiation and rear surface temperature. Moreover, the lower mass flow rate at $\dot{m}_1$ weakens convective heat transfer and increases the thickness of the thermal boundary layer near the rear surface. This can result in non-uniform cooling during the injection time. As a result, the rear surface may see alternate periods of absorbing heat during gas injection and partial temperature recovery after the cooling effect diminishes, leading to fluctuations in the calculated values of Q. In contrast, at $\dot{m}_2$ and especially $\dot{m}_3$, the higher mass flow rate of the secondary and tertiary airflow, combined with the lower temperature of the injected gas, gives stronger, more stable thermal contact with the rear surface — and thus smoother, higher rates of heat removal.

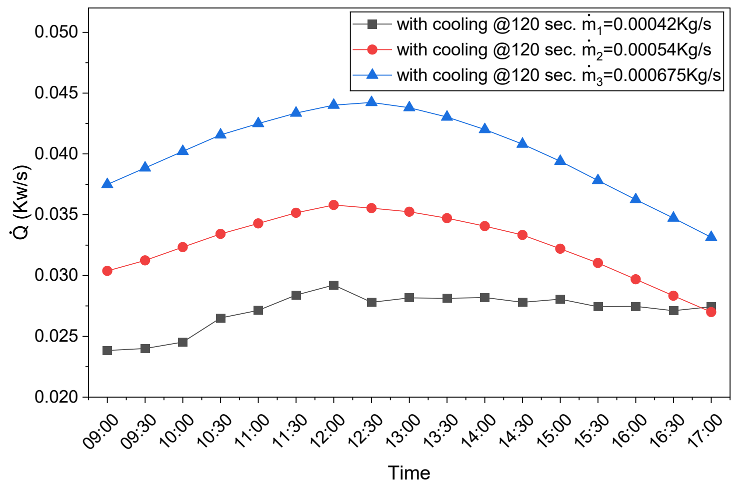

Figurer 20. Effect of mass flow rate on heat removal rate at 120 – second injection duration.

Figure 21 shows the results of the effect of injection duration on the heat removal rate Q at a constant mass flow rate of $\dot{m}_2$ = 0.00054 kg/s. Three injection durations were considered: 60 seconds, 90 seconds, and 120 seconds. The results of this study indicated that Q increased gradually during the morning hours due to the increase in solar radiation and the thermal load on the rear surface of the PV panel and then decreased in the afternoon as solar radiation declined. The maximum heat removal rate was 0.01785 kW/s at 60 seconds, which increased to 0.03407 kW/s at 90 seconds and to 0.03549 kW/s at 120 seconds. An increase in Q with longer injection duration can be explained by the fact that the cold gas has more time to stay in contact with the rear surface, hence enhancing convective heat transfer, and making the gas more capable of absorbing and carrying heat away from the panel. The results also show that the improvement from 60 seconds to 90 seconds was more significant than the improvement from 90 seconds to 120 seconds. On average, Q was about 0.03116 kW/s at 90 seconds and 0.03229 kW/s at 120 seconds. Additional thermal benefit becomes limited after 90 seconds. Therefore, the 120-second duration was the best thermal performer, while the 90-second duration could be a practical option in the trade-off of heat removal enhancement and injected gas consumption.

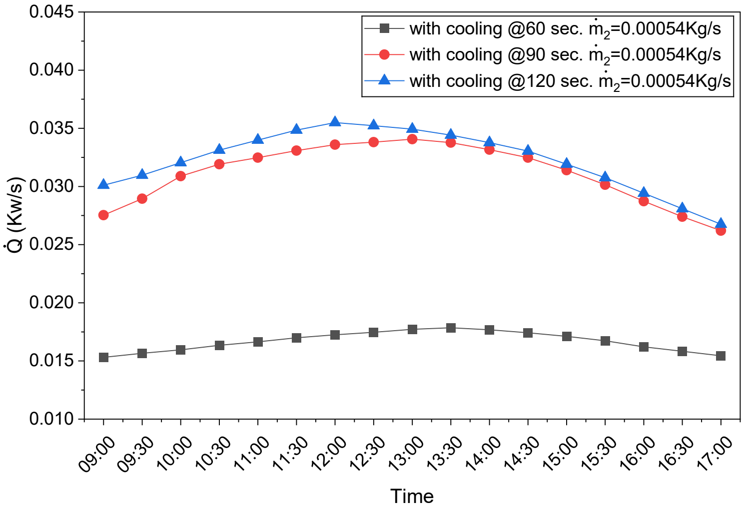

Figure 21. Effect of injection duration on heat removal rate at $\dot{m}_2 = 0.00054\ Kg/s$

5.9 Electrical Efficiency performance analysis

Figure 22 shows the results of rear surface cooling on the electrical efficiency of the photovoltaic panel for an injection duration of 60 seconds and a mass flow rate of $\dot{m}_3$ = 0.000675 kg/s. The electrical performance of the cooled panel was always superior to that of the uncooled panel during the tests. The efficiency of the cooled panel was from about 19.565% to 22.2% while the efficiency of the uncooled panel went from 18.292% to 20.8%. It grew from 19.102% without cooling to 20.426% with cooling, a gain of 1.324 percentage points on average or 6.93%. The improvement is since the cold gas injected over the rear surface lowers the operating temperature of the PV panel. That is, the average electrical efficiency was improved from about 19.102% without cooling to 20.426% with cooling, which is an average increase of 1.324 percentage points or approximately 6.93%. A high cell temperature results in high thermal losses and low efficiency of photovoltaic conversion, and cooling on the rear surface improves the thermal state of solar cells and thus high electrical efficiency.

Moreover, the high mass flow rate $\dot{m}_3$ and the lower injected gas temperature further increase the temperature difference between the heated rear surface and the cooling gas, so further improve the cooling effect. Therefore, these results prove that rear-surface cooling at m3 and 60-second injection duration not only decreases the panel temperature and enhances the output power but also directly improves the electrical efficiency, which is the most important indicator for the evaluation of photovoltaic panel performance.

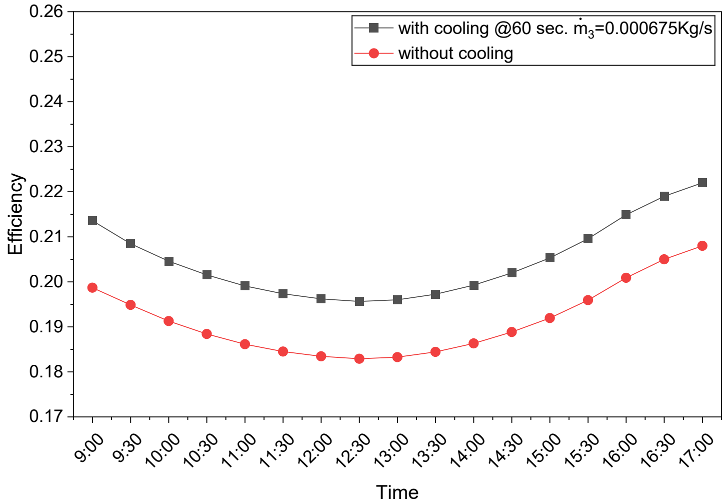

Figure 22. Effect of rear surface cooling on electrical efficiency at 60 – second injection duration and $\dot{m}_3$ mass flow rate.

As illustrated in Figure 23, the results depict the influence of rear-surface cooling on the electrical efficiency of the photovoltaic panel at an injection duration of 120 seconds and a mass flow rate of $\dot{m}_3$ = 0.000675 kg/s. It can be seen from the results that the cooled panel achieved higher electrical efficiency than the uncooled panel throughout the testing period. Electrical efficiency under cooling ranged from approximately 21.10% to 22.00%, while that of the uncooled panel ranged from about 19.23% to 20.16%. The average efficiency increased from 19.65% without cooling to 21.49% with cooling, giving an average enhancement of about 1.84 percentage points, equivalent to an improvement of approximately 9.36%. This enhancement represents the strongest efficiency enhancement because the combination of the longest injection duration and the highest mass flow rate provided more effective thermal control of the PV panel. This test result is also in line with a previous study where an enhancement of about 9% was realized in a similar PV panel when lower mass flow rates were used. The injected cold gas stayed in contact with the rear surface for a longer time; the higher mass flow rate increased the amount of cooling gas over the heated surface, too. As a result, heat accumulation was more effectively reduced, and solar cells operated under lower thermal stress. Since electrical efficiency is very sensitive to the operating temperature of PV cells, the reduction in rear surface temperature assisted in limiting thermal losses while improving photovoltaic conversion performance. Therefore, rear surface cooling at 120 seconds and $\dot{m}_3$ = 0.000675 kg/s can be considered the best condition for improving the electrical efficiency of the photovoltaic panel.

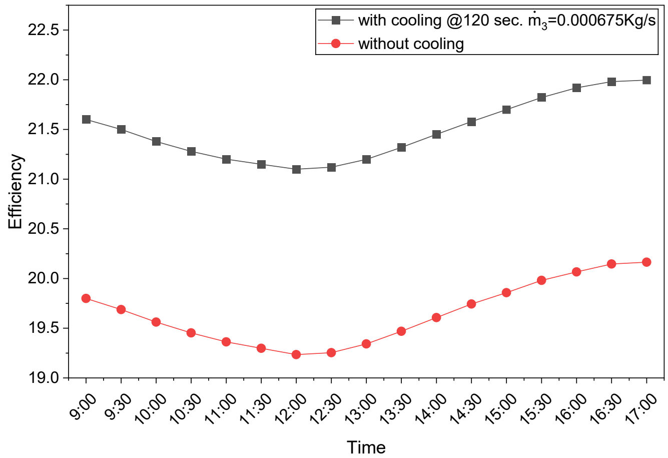

Figure 23. Effect of rear surface cooling on electrical efficiency at 120 – second injection duration and $\dot{m}_3$ mass flow rate.

5.10 Effect of mass flow rate on average electrical efficiency

Figure 24 shows the average electrical efficiency of the photovoltaic panel at three different mass flow rates under a constant injection duration of 60 seconds. These were $\dot{m}_1$ = 0.00042 kg/s, $\dot{m}_2$ = 0.00054 kg/s, and $\dot{m}_3$ = 0.000675 kg/s. The average electrical efficiency was found to be 19.653% for m1, 19.968% for m2 and 20.481% for $\dot{m}_3$. This shows that the increase in the mass flow rate improves the cooling effectiveness and improves the average electrical efficiency of the photovoltaic panel. The improvement is attributed to the combined effect of increasing the mass flow rate and decreasing the injected gas temperature at m1 the temperature of the injected gas was −18 °C, which decreased to −25 °C at m2 and to −35 °C at m3. Thus, $\dot{m}_3$ supplied more cold gas over the rear surface and increased the temperature difference between the heated panel and the injected gas, which increased the convective heat transfer. This in turn resulted in less heat accumulation and thus better photovoltaic conversion performance. Thus, $\dot{m}_3$ had the highest mean electrical efficiency and was in the best condition at the 60-second injection duration. This also confirms that the highest mass flow rate was the most effective condition for the injection duration of 60 seconds.

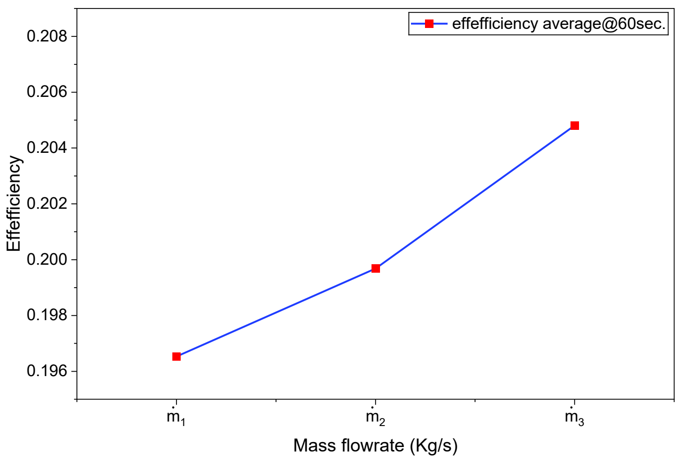

Figure 24. Average electrical efficiency at different mass flow rate for 60 – second injection duration.

5.11 Effect of injection duration on average electrical efficiency

Figure 25 illustrates the results of average electrical efficiency for the photovoltaic panel at a constant mass flow rate of $\dot{m}_2$ = 0.00054 kg/s for different injection durations. Three injection durations were considered, 60 seconds, 90 seconds, and 120 seconds. The average electrical efficiency was 19.968% at 60 seconds, 20.362% at 90 seconds, and 21.343% at 120 seconds. Such a trend clearly shows that enhancing the injection duration improved the effectiveness of cooling and hence the average electrical efficiency for the photovoltaic panel. The better results can be ascribed to the increased contact time between the injected cooling gas and the rear surface of the PV panel. More time permits the cooling gas to absorb more heat from the hot rear surface, thus reducing the buildup of heat and enhancing the thermal operating conditions of the solar cells. Going from 60 seconds to 120 seconds boosted absolute efficiency by about 1.375 percentage points — or close to 6.89% better. So, the 120-second duration reached the highest average electrical efficiency at $\dot{m}_2$, proving that increasing injection time is a good way to boost PV performance at this mass flow rate.

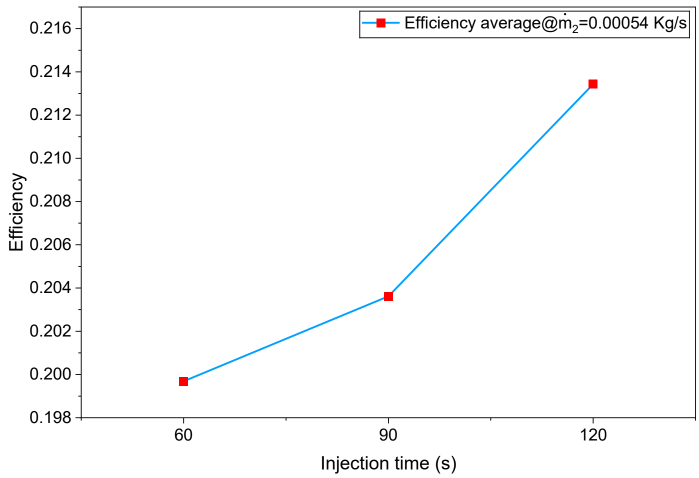

Figure 25. Average electrical efficiency at different injection duration for $\dot{m}_2$=0.00054 Kg/s

5.12 Comparison of dimensionless temperature reduction and power improvement between clean and unclean CO_2 cooled PV modules

Figure 26: Variation of dimensionless temperature reduction with time for a (CO_2) mass flow rate of ($\dot{m}$ = 0.00042 kg/s) and injection of 90 s. Two cases were compared, the first case is the clean cooled PV module compared with the clean uncooled reference module and the second case is the unclean cooled PV module compared with the clean uncooled reference module. Generally, the clean cooled PV module showed more dimensionless temperature reduction than the unclean cooled PV module for most of the testing time. In the clean cooled case, the maximum value of ($\Delta T/T$) was around 0.08904 i.e. around 8.90% at 12:00 PM. In contrast, the maximum for the unclean cooled case was about 0.07598, which corresponds to about 7.60% at the same time. This implies that the effect of cleaning and cooling together would give better thermal reduction than cooling the unclean module.

The average dimensionless temperature reduction was 0.0718 in the clean cooled module and 0.0661 in the unclean cooled module. This means that the clean cooled case achieved a slightly higher average temperature reduction, which was about 0.57 percentage point better than the unclean cooled case. This can be explained by the fact that the clean PV surface exhibits a more uniform thermal behavior while the presence of dust could induce non-uniform heating and reduce the effective thermal response of the module.

In the late afternoon, the difference between the two cases became small and the curves became close to each other. This is mainly caused by the decrease of solar irradiance during this period, so the thermal load on the PV module will be lower. As a result, the effect of cleaning and cooling is less pronounced than at around midday. Thus, the clean cooled PV module showed better thermal behavior, especially during the period of high solar radiation around noon.

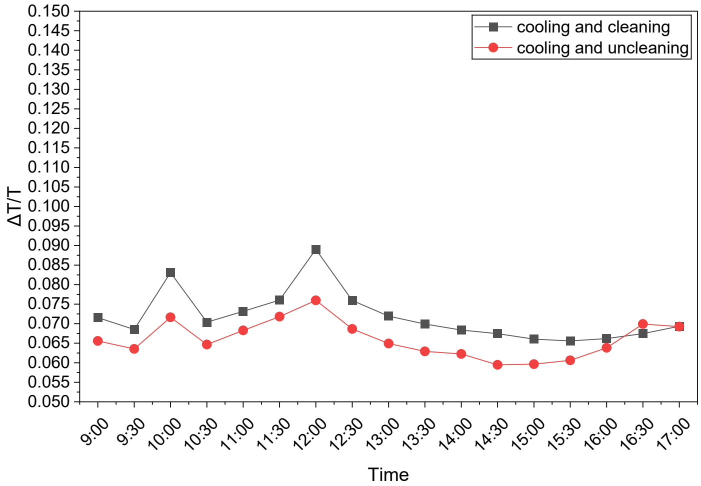

Figure 26. Dimensionless temperature reduction versus time for clean and unclean CO_2- cooled PV modules.

Figure 27. Dimensionless power improvement with time for a mass flow rate of (CO_2) $\dot{m}$ = 0.00042 kg/s and injection duration (90 s). Two comparisons were conducted, clean cooled PV module vs. clean uncooled reference module and unclean cooled PV module vs. clean uncooled reference module.

The electrical power increased more steadily for the clean cooled PV module over most of the testing period. The value of ($\Delta P/P$) was found to be close to 0.065 for most of the operating time, that is close to 6.5%. This shows that the combined cleaning and rear-side cooling achieved a stable increase in output power by reducing the impact of dust accumulation and the module temperature.

The dimensionless power improvement values for the unclean cooled PV module were lower in the morning and midday periods with respect to the clean cooled case. This can occur due to the dust accumulated on the surface of the module that reduces the solar radiation reaching the PV cells. Thus, the effect of the dust limited the improvement of electrical power even if the rear-side cooling was applied as compared to the clean cooled module.

The average dimensionless power gain was approximately 0.0661 (6.61%) for the clean cooled module and approximately 0.0432 (4.32%) for the unclean cooled module. This shows that the clean cooled case has achieved a higher power improvement of about 2.29 percentage points in comparison with the unclean cooled case.

At the end of the test period, the unclean cooled case values increased noticeably and were close to or above some values of the clean cooled case. This does not imply that the unclean module is superior to the clean module. But it can be related to the nature of the dimensionless calculation, where the improvement ratio becomes more sensitive as the reference power decreases in the late afternoon due to the reduction of the solar irradiance. The late-time values should be taken with caution, and the general trend and average values should be considered.

According to these results, the clean cooled PV module presented the best overall electrical performance as it combines the benefits of reducing losses due to dust and improving thermal regulation on the rear side.

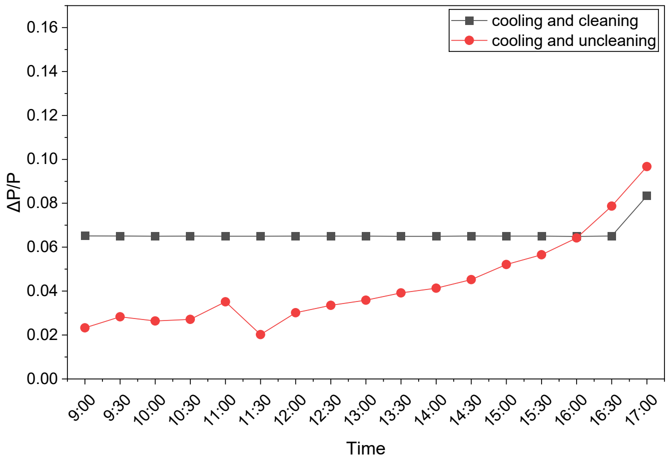

Figure 27. Dimensionless power improvement versus time for clean and unclean CO_2-cooled PV modules.

5.13 Overall discussion and best operation condition

Results obtained clearly indicate that rear surface cooling enhances the thermal as well as electrical performance of the photovoltaic panel. The lower temperature of the rear surface led to better thermal regulation of the PV cells, which was reflected in higher electrical power with improved electrical efficiency. Results also indicated that injection duration and mass flow rate were two major parameters for controlling the effectiveness of the cooling. Increasing injection duration from 60 seconds to 120 seconds increased the performance of the cooling, while an increase in mass flow rate increased convective heat transfer because more cooling gas was passing over the rear surface. Out of all the tested conditions, the best overall performance was achieved at the highest mass flow rate of $\dot{m}_3$ = 0.000675 kg/s, which also happened to be at the longest injection duration of 120 seconds. This condition was the best from the point of view of thermal management because it allowed the most cooling gas to be used and the longest contact time between the gas and the rear surface of the panel. Furthermore, the lower injected gas temperature at m3 increased the temperature difference between the heated panel surface and the cooling gas, thus improving heat removal and reducing heat accumulation. In the end, this condition resulted in the lowest rear surface temperature, highest heat removal rate, and best improvement in electrical efficiency. The best thermal and electrical performance was achieved for the 120-second injection duration. However, results also show that the 90-second injection duration can be a reasonable alternative in the trade-off between performance improvement and cooling gas consumption. The difference between the two cases of 90 seconds and 120 seconds was smaller than the improvement of going from 60 seconds to 90 seconds. Therefore, the optimal operating condition would depend on the priority of the system. For maximum performance, $\dot{m}_3$ should be used at 120 seconds, while $\dot{m}_3$ at 90 seconds may be suitable when reducing coolant consumption is considered equally important. In general, the results of the experiments prove rear surface cooling to be a good method in improving photovoltaic (PV) panel performance under high temperature of the operation. The best operating point in this study was obtained at $\dot{m}_3$=0.000675 kg/s and an injection duration of 120 seconds which provided superior thermal regulation and improved the electrical efficiency of the PV panel.

5.14 Summary

In this chapter the results of the experiments performed and their discussion about when rear-surface cooling is applied to photovoltaic panels are presented. This includes the variation of solar radiation and ambient temperature, rear surface temperature, electrical output power, heat removal rate and electrical efficiency under various operating conditions. The results indicate that the rear-surface cooling reduced the operating temperature of the PV panel and enhanced its thermal performance in comparison with the uncooled case. The results also show that the cooling performance can be improved by increasing both the injection duration and the mass flow rate. Higher mass flow rates increase the amount of cooling gas above the heated surface. Longer injection times increase the contact time between the cooling gas and the rear surface. As a result, better heat removal, higher output power and improved electrical efficiency were obtained. The highest performance in the experiments was achieved at the highest mass flow rate $\dot{m}_3$ = 0.000675 kg/s with injection time of 120 seconds. Also, comparison of the results obtained under cooling and cleaning conditions indicated that surface cleaning enhances the optical performance of the panel while rear-surface cooling improves its thermal behavior. Combining both processes would result in an overall improved photovoltaic performance. The results, in general, confirm the rear-surface cooling as an effective technique for improving the performance of photovoltaic panels.

Conclusion

1- The experimental study investigates the impact of rear side cooling of a photovoltaic module by using carbon dioxide (CO_2) gas.
2- The experiments were performed at different mass flow rates and injection times of (CO_2) to study their effects on the thermal and electrical performance of the PV module.

3- The effect of temperature rise on PV performance was successfully analyzed, the rear-side (CO_2) cooling system was designed and implemented, the temperature of the module before and after cooling was measured, and the improvement in output power and electrical efficiency was evaluated.
4- The results indicated that the higher operating temperature of the PV module has a negative impact on the electrical performance of the PV.
5- The cooled PV module showed lower temperatures than the uncooled reference

module, which confirms the effectiveness of the proposed rear-side (CO_2) cooling system.

6- The average temperature reduction increased from about (2.48 ºC) to (6.15 ºC) when the injection duration increased from 60 s to 120 s to improve the cooling effect.

7- The increase of the (CO_2) mass flow rate from ($\dot{m}_1$= 0.00042 kg/s) to ($\dot{m}_3$= 0.000675;kg/s) improved the forced convective heat transfer and the heat removal from the rear surface of the PV module.

8- The rear-side (CO_2) cooling enhanced both the output power and the electrical efficiency of the PV module.

9- The average power improvement increased from approximately 5.27% at an injection duration of 60 s to approximately 8.64% at 120 s.

10- The maximum average electrical efficiency was achieved at the mass flow rate of (CO_2) of (0.000675 kg/s) and the injection time of 120 s.

11. The electrical efficiency increased from 19.65% for the uncooled module to 21.49% for the cooled module under the best operating condition, an increase of about 9.36%.

12- The comparison between the cooled and uncooled PV modules showed that the rear-side (CO_2) cooling can effectively reduce the heat accumulation and improve the thermal and electrical performance of PV modules under the hot outdoor climatic conditions.

13- The best performance reached at the highest mass flow rate and the longest injection time in the range of this study.

14- The results clearly showed the relationship between reducing PV module temperature and increasing output power and electrical efficiency.

15- The results of this study may aid the future development of gas-based cooling methods for thermal management of photovoltaic.

REFERENCES

Abdulridha, Z.S. *et al.* (2025) "SIMULATION OF AN ENERGY-GENERATING HOME CANOPY USING PHOTOVOLTAIC PANELS WITH," 16(4).

Abed, R.H. (2024) "INVESTIGATION OF HYBRID PHOTOVOLTAIC / THERMAL SOLAR SYSTEM PERFORMANCE UNDER IRAQ ' S CLIMATE CONDITIONS," 15(1), pp. 1–18.

Ahmed, S. *et al.* (2022) "Enhanced radiative cooling of solar cells by integration with heat pipe," *Applied Energy*, 308(February). Available at: https://doi.org/10.1016/j.apenergy.2021.118363.

Al-jabari, A.R., Korkmaz, F. and Teke, M. (2022) "A SIMULATION OF STAND-ALONE SOLAR ENERGY SYSTEM CONTROLLED BY P & O , IC , AND FUZZY LOGIC," 13(3), pp. 41–58.

Azmi, M.S.F.M. *et al.* (2023) "Hybrid Cooling System for Solar Photovoltaic Panel," *Journal of Physics: Conference Series*, 2550(1). Available at: https://doi.org/10.1088/1742-6596/2550/1/012004.

Basem, A. *et al.* (2024) "Experimental study on the various varieties of photovoltaic panels (PVs) cooling systems to increase their electrical efficiency," *PLoS ONE*, 19(9 Septeber), pp. 1–24. Available at: https://doi.org/10.1371/journal.pone.0307616.

Chaudhary, T.N. *et al.* (2024) "Experimental and Performance Evaluation of the Soiling and Cooling Effect on the Solar Photovoltaic Modules," *Arabian Journal for Science and Engineering*, 49(2), pp. 1421–1432. Available at: https://doi.org/10.1007/s13369-023-07858-x.

Eid, A.F. *et al.* (2022) "Hybrid cooling techniques to improve the performance of solar photovoltaic modules," *Solar Energy*, 245(September), pp. 254–264. Available at: https://doi.org/10.1016/j.solener.2022.09.026.

Harmailil, I.O. *et al.* (2024) "The State of the Art of Photovoltaic Module Cooling Techniques and Performance Assessment Methods," *Symmetry*, 16(4). Available at: https://doi.org/10.3390/sym16040412.

Jain, P.K. *et al.* (2026) "Thermal analysis of flat plate solar air heater system with radiation reflectors and W-shaped roughness : artificial neural network & machine learning approach," pp. 1–20.

Jasim, Q.K. (2023) "Studying the Effect of Cooling Methods on the Performance of Solar Cells," *International Journal of Heat and Technology*, 41(1), pp. 265–270. Available at: https://doi.org/10.18280/ijht.410130.

KARAOZAN, Ö. and ASKER, M.E. (2023) "Changes in The Electrical Output Power and Efficiency of A Photovoltaic Panel Cooled by A Hybrid Method," *European Journal of Technic*, 13(2), pp. 164–173. Available at: https://doi.org/10.36222/ejt.1404493.

Lebbi, M. *et al.* (2021) "Energy performance improvement of a new hybrid PV/T Bi-fluid system using active cooling and self-cleaning: Experimental study," *Applied Thermal Engineering*, 182, p. 116033. Available at: https://doi.org/10.1016/j.applthermaleng.2020.116033.

Mizani, S., Khoshvaght-aliabadi, M. and Tae, Y. (2025) "Enhancing thermal management in concentrated photovoltaic cells using supercritical carbon dioxide," *Applied Thermal Engineering*, 274(PA), p. 126555. Available at: https://doi.org/10.1016/j.applthermaleng.2025.126555.

Nabil, T. and Mansour, T.M. (2022) "Augmenting the performance of photovoltaic panel by decreasing its temperature using various cooling techniques," *Results in Engineering*, 15(August), p. 100564. Available at: https://doi.org/10.1016/j.rineng.2022.100564.

Paradis, P. *et al.* (2018) "A hybrid PV / T solar evaporator using CO 2 : Numerical heat transfer model and simulation results," *Solar Energy*, 170(May), pp. 1118–1129. Available at: https://doi.org/10.1016/j.solener.2018.06.015.

Pichandi, R. *et al.* (2024) "Performance enhancement of photovoltaic module by integrating eutectic inorganic phase change material," *Energy Sources, Part A: Recovery, Utilization and Environmental Effects*, 46(1), pp. 16360–16377. Available at: https://doi.org/10.1080/15567036.2020.1817185.

Popovici, C.G. *et al.* (2016) “Efficiency Improvement of Photovoltaic Panels by Using Air Cooled Heat Sinks,” *Energy Procedia*, 85(November 2015), pp. 425–432. Available at: https://doi.org/10.1016/j.egypro.2015.12.223.

Prakash, A., Kukreja, R. and Kumar, P. (2025) “Improving the performance of PV panel by using PCM with nanoparticles and Bifluid-A comprehensive review,” *Materials Chemistry and Physics: Sustainability and Energy*, 2(December 2024), p. 100005. Available at: https://doi.org/10.1016/j.macse.2024.100005.

Refaey, H.A. *et al.* (2021) “Experimental Study on the Performance Enhancement of the Photovoltaic Cells by Using Various Nano-Enhanced PCMs,” *Journal of The Institution of Engineers (India): Series C*, 102(2), pp. 553–562. Available at: https://doi.org/10.1007/s40032-020-00655-7.

Al Sadoon, A.M., Kassim, M.S. and Mohmood, R.A. (2024) “Comparative Study of Cooling Techniques for Photovoltaic Panels: Active Cooling Techniques, A Review,” *Journal of Engineering and Sustainable Development*, 28(5), pp. 580–592. Available at: https://doi.org/10.31272/jeasd.28.5.3.

Tables, P. (no date) “Appendix 1,” pp. 909–999.

Verma, K. *et al.* (2023) “Photovoltaic Panel Integration Using Phase Change Material (PCM): Review,” *Evergreen*, 10(1), pp. 444–453. Available at: https://doi.org/10.5109/6782147.

Xu, Z. *et al.* (2023) “Cooling characteristics of solar photovoltaic panels based on phase change materials,” *Case Studies in Thermal Engineering*, 41(September 2022), p. 102667. Available at: https://doi.org/10.1016/j.csite.2022.102667.

Zanetti, E., Bordignon, S., *et al.* (2023) “Experimental and numerical analysis of a CO 2 dual-source heat pump with PVT evaporators for residential heating applications,” *Applied Thermal Engineering*, 233(May), p. 121165. Available at: https://doi.org/10.1016/j.applthermaleng.2023.121165.

Zanetti, E., Azzolin, M., *et al.* (2023) “Performance and control of a CO 2 dual source solar assisted heat pump with a photovoltaic-thermal evaporator,” *Applied Thermal Engineering*, 218(September 2022), p. 119286. Available at: https://doi.org/10.1016/j.applthermaleng.2022.119286.

Zhang, W. *et al.* (2024) “Modeling Heat Mitigation in Hollow-Core Gas Fiber Lasers With Gas Flow,” *IEEE Journal of Selected Topics in Quantum Electronics*, 30(6), pp. 1–8. Available at: https://doi.org/10.1109/JSTQE.2024.3430929.